Nuclear Science and Techniques **24** (2013) 020201

Swelling and thermal properties of porous PNIPAM/PEG hydrogels prepared by radiation polymerization

LI Zhihui[1] LIU Wentao[1,*] LI Zhongyuan[2] YANG Mingcheng[3] GAO Xujing[1]
CUI Haitao[1] HE Suqin[1] ZHU Chengshen[1]

[1]*School of Materials Science and Engineering, Zhengzhou University, Zhengzhou 450052, China*

[2]*Shenzhen Academy of Metrology& Quality Inspection, Shenzhen 518131, China*

[3]*Isotope Institute of Henan Academy of Sciences, Zhengzhou 450015, China*

Abstract In this study, a series of porous intelligent hydrogels were synthesized by radiation exhibiting the lower critical solution temperature (LCST) and fast response involving a combination of *N*-isopropyl acrylamideas monomer, polyethylene glycol (PEG) as pore-forming agent and *N*,*N*-methylene-bis-acrylamide as crosslinking agent. The hydrogels were analyzed by Fourier transform infrared spectroscopy, and the influence of radiation doses on their swelling and thermal behaviors were studied. Their surface morphologies were examined by scanning electron microscopy. The results showed that PEG molecules only acted as pore-forming agent in the cross-linked polymerization. Their swelling ratios reduced with increasing radiation doses. The LCST was around 37°C, and varied little with the radiation doses. The frozen water content of PNIPAM/PEG_{6000} hydrogel reduced with increasing the radiation dose, and was greater than that of PNIPAM hydrogel at 15 kGy. Hydrogel macropores were prepared by PEG agent, and the hydrogels without PEG had a dense surface. The porous hydrogels are expected to be applied in the field of artificial intelligence material.

Key words PNIPAM, Swelling properties, Thermal properties, Radiation

1 Introduction

Hydrogel, a hydrophilic polymer network, can absorb a large amount of water or other biological fluid, but are insoluble because their molecules are cross-linked into a three-dimensional network[1]. Also, the stimuli-sensitive hydrogels have the capability to change their swelling behavior, permeability or mechanical strength in response to external stimuli, such as small changes in pH[2], ionic strength[3], temperature[4], light sensitivity[5], and electromagnetic radiation[6]. These hydrogels have numerous applications, particularly in medical and pharmaceutical fields[7]. As the most promising biomaterial, they may be applied in the contact lens[8], burn dressings[9], artificial corneas[10], soft tissues substances[11], separation analysis[12], tissue engineering[13], and immobilized enzyme[14].

Up to now, these applications are limited by their low efficiency and slow rate of response. The rapid response PNIPAM hydrogels have been prepared by many methods, such as the introduction of dynamic graft chains[15], freezing[16], the interpenetrating network structure[17]. The efficiency and the response rate of hydrogels to external stimuli can be controlled by the degree of porosity. The porosity plays role in enhancing the total water sorption capability and the response rate by reducing the transport resistance. Therefore, porosity creating in hydrogels has been considered as an important process in many ways. Except the phase-separation technique[18], the water soluble porogen technique[19], and the foaming technique[20], another method preparing porous hydrogels is to use pores in the matrix. The porous structure facilitates the water migrating through the

Supported by the Key Science and Technology Project of Henan Province (No. 102101210100) and the Natural Science Foundation of Henan Province (No. 2011 B430023)

* Corresponding author. *E-mail address*: wtliu@zzu.edu.cn

Received date: 2012-07-20

large surface area contained within the pores. The preparation of porous hydrogels has been described by several literatures, including the surfactant incorporation and their subsequent extraction[21], freeze drying[22], and gas forming[23].

The PNIPAM hydrogels can be prepared by chemical polymerization, radiation-induced polymerization and interpenetrating polymer network, and modified by gamma radiation-induced polymerization under sterilisation without initiators or cross-linking agents[24].

In this paper, the PNIPAM/PEG hydrogels are prepared by radiation polymerization using *N*-isopropyl acrylamide (NIPAM) as monomer, and polyethylene glycol (PEG) as pore-forming agent. The influence of radiation doses on its swelling and thermal properties is discussed. The porous PNIPAM/PEG hydrogels are appropriate as release polymer systems in pharmaceutical formulations.

2 Materials and methods

2.1 Materials

NIPAM (AR, Tokyo Chemical Industry beads Clubs), *N*,*N*-methylene-bis-acrylamide (MBA,AR, Tianjin Kermel Chemical Reagent Development Center), PEG(AR, Shanghai Pharmaceutical Group Chemical Reagent Co, Ltd.).

2.2 The PNIPAM/PEG hydrogels preparing at different radiation doses

The NIPAM monomer, MBA (2 wt%), PEG (10 wt%, M_n=6000) were dissolved by water. All the monomers were 5 wt% in the pregel solution. The dissolved oxygen in the solvent was removed by bubbling nitrogen gas for 10 min, and sealed into tubes before irradiation at room temperature. Radiation polymerization was carried out by the 8-, 15-, and 22-kGy radiation doses at the 5 kGy/h. The activity of ^{60}Co-γ ray radioactive sources (Institute of Isotopes Henan Academy of Sciences) is 7.4×10^{15} Bq. After radiation, the tubes were removed and placed for two days. Then samples from the tubes were cut into thin slices of about 3-mm thickness, and soaked in deionized water for 3 days under changing the water every day, to remove the residual monomers and pore-forming agent. Finally, the samples were dried to constant weight under vacuum. Similarly, the PNIPAM hydrogels were homopolymerized by the NIPAM monomer, MBA (2 wt%) and deionized water(10 mL).

2.3 Determination of swelling kinetics of hydrogels

Swelling properties of hydrogels were studied by the equilibrium swelling ratio which was measured by the classical gravimetric method. The hydrogels were dried in a 50°C vacuum oven for 24 h to weigh in the dried state (m_0). Then, the samples were immersed in deionized water at 25°C, and taken out at every end of interval. Finally, the excess water on their surface was wiped quickly by gauze and weighing. After equilibrating process several times, if the gel sample remained constant weight, it was regarded as the weight in an equilibrium state (m_t) at the time of the interval (t). Each sample was measured three times to take its average value. The swelling ratio (SR) was defined as

$$SR = (m_t - m_0)/m_0 \quad (1)$$

2.4 Determination of equilibrium swelling and de-swelling kinetics

Equilibrium swelling ratio (SR_e) of hydrogels is defined as

$$SR_e = (m_e - m_0)/m_0 \quad (2)$$

where m_e is the hydrogel weight reaching equilibrium swelling at certain temperature.

The volume phase transition characteristics as temperature sensitivity is test as follows: The dried hydrogels were immersed in deionized water at the temperatures of 25°C to 55°C, which covered the expected range of the lower critical solution temperature (LCST). At each predetermined temperature, the hydrogel samples were allowed to swell for over 24 h, weighed until their constant weight after wiping the excess water on their surface quickly by gauze. After measuring weight, the hydrogels were three times re-equilibrated in water at another predetermined temperature, and weighed as above to take their average value. From the plot of swelling ratio vs. temperature, the LCST was determined as the temperature point where the swelling ratio curve reaches the plateau.

De-swelling behavior was measured beyond LCST after the hydrogel had reached swelling equilibrium at 25°C. The gravimetric method was also employed to study their temperature response kinetics. After weighing m_e, the sample was immersed in the water bath of 50°C. At the predetermined time intervals, the hydrogels were taken out and weighed after removing the excess water on its surface with gauze. The absorbed water at each temperature was calculated. Each sample was weighed three times to take its average value. The water loss rate (LR_w) was deduced from Eq.(3).

$$LR_w = (m_{25}-m_t)/m_{25}\times 100\% \quad (3)$$

where m_{25} is the water weight absorbed by hydrogel reaching swelling equilibrium at 25°C, m_t is the water weight absorbed by hydrogel at 50°C.

2.5 Determination of the gel fraction

The gel fraction was measured by the classical gravimetric method. Hydrogels drying to constant weight (m_0) in the vacuum oven were placed in boiling distilled water for 4 h, and repeatedly washed with deionized water to remove the sol. Again, the hydrogel was dried to constant weight (m). Each sample was measured three times. The gel fraction (G_f) was deduced by Eq.(4).

$$G_f = (m/m_0)\times 100\% \quad (4)$$

2.6 Fourier transform infrared spectroscopy (FTIR) analysis

Hydrogel samples were dried completely, ground to fine power, and pressed pellet embedded in KBr. Infrared absorption spectra were recorded with Nicolet PROTE/GE/ 460 in the range of 400–4000 cm^{-1}.

2.7 Differential scanning calorimetry analysis

The frozen and non-frozen water of hydrogels could be determined by differential scanning calorimetry (DSC). The hydrogels in the state of equilibrium swelling at 20°C was cut into a sample of about 15 mg. The sealed empty sample pan were weighed and quickly frozen to –30°C inside the DSC chamber. The DSC was conducted with STA449C integrated thermal analyzer of NETZSCH company Germany-based to test their volume phase transition behavior and the process of water evaporation at the heating rate of 2°C /min under nitrogen atmosphere.

2.8 Thermal gravimetric (TG) analysis

Thermal stability of hydrogels was valued by DSC. The samples about 20 mg was dried to a constant weight in vacuum, moved to a sample pan, and recorded on a STA449C TG (NETZCH Co.) in the range of 30–500°C at heating rate at 10°C /min.

2.9 Scanning electron microscopy (SEM) analysis

The surface morphology of the hydrogels was investigated by SEM. Hydrogels were swollen completely in deionized water at 25°C, and freeze-dried for 15 h to avoid the collapse of porous structure. The freeze-dried samples were fractured carefully, mounted onto aluminium stubs, and coated with gold. Finally, their surface morphologies were determined by a JSM-5610LV SEM (JEOL Corporation, Japan).

3 Results and Discussion

3.1 IR spectra of hydrogels

Figure 1 shows FTIR spectra of PNIPAM and PNIPAM/PEG hydrogels at 15-kGy radiation dose. Both the spectra of hydrogels were similar with each other. The absorption band at 3200–3600 cm^{-1} was attributed to the stretching vibration of -OH and -NH. A typical band of saturation of C-H vibration had the similar intensity at 2800–3000 cm^{-1} at each curve.

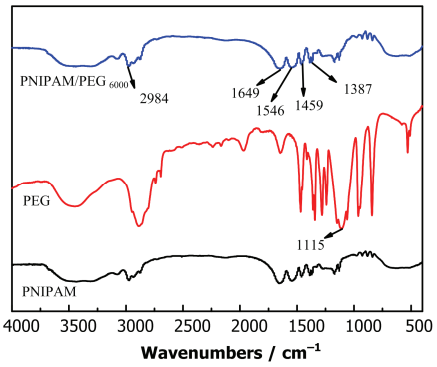

Fig.1 FTIR spectra of the PNIPAM and PNIPAM/PEG hydrogels at the radiation dose of 15 kGy.

Each spectrum exhibits amide Ⅰ band at 1649 cm^{-1} of C=O stretch of PNIPAM and amide Ⅱ band at

1546 cm^{-1} of N-H rocking. The absorption band at 1387 cm^{-1} and 1459 cm^{-1} were assigned to -CH $(CH_3)_2$ absorption. There was no the typical C-O-C absorption of PEG molecule at 1050–1150 cm^{-1}, indicating that the PEG molecules as pore-forming agent in the process of cross-linked polymerization did not participate in the reaction.

3.2 The dependence of the swelling properties of hydrogels on radiation doses

Figure 2 shows the swelling kinetics behaviors of PNIPAM/PEG_{6000} hydrogel at different radiation doses at 25°C, their swelling ratio increases with the swelling time, and tends to balance after more than 30 h. Meanwhile, the *SR* decreases with increasing the radiation dose.

In Table 1, the gel fraction increases with the radiation dose. The energy intensity in polymerization process increases with the radiation dose, causing a more complete monomer polymerization. Cross-linking density increases to form more fully cross-linked polymer. The SR_e is determined by the three factors[25]. (1) The mixing free energy of network segments and solvent molecules. (2) The osmotic pressure is caused by counter ion charges when the network segment charged to maintain electrical neutrality. (3) The osmotic pressure is caused by their elongated chain swellings.

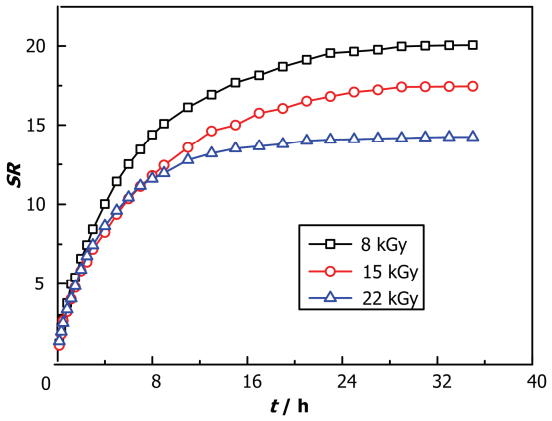

Fig.2 The swelling kinetics of PNIPAM/PEG_{6000} hydrogel at different radiation doses.

Table1 Gels fraction of PNIPAM/PEG_{6000} hydrogel at different radiation doses

Radiation dose / kGy	Sample 1 G_{f1}/ %	Sample 2 G_{f2}/ %	Sample 3 G_{f3}/ %	Sample 4 G_{f4}/ %	Sample 5 G_{f5}/ %	Average gel fraction G_f/ %
8	84.7	84.1	83.8	84.2	84.6	84.3
15	91.7	90.5	91.0	90.6	89.8	90.7
22	96.0	95.9	96.2	96.4	96.2	96.2

The quantitative relationship of cross-linked degree with absorbed dose is derived by Charles[26].

$$s+s^{0.5}=[p_0/q_0]+2q_0^{-1}\mu_{2.0}^{-1}R^{-1} \quad (5)$$

where, *g* is the gel fraction, *s* is the sol fraction, $s=1-g$; p_0 is the cracked degree and q_0 is cross-linked degree for a unit dose at 1 kGy, $u_{2.0}$ is weight average molecular weight, *R* is the radiation dose.

In a certain range of radiation dose, the *g* of PNIPAM/PEG_{6000} hydrogel increases with the radiation dose, resulting in elastic restoring force of network, and the osmotic pressure between inside and outside of hydrogel declines. In Eq.(5), the q_0 increases with the radiation dose. The SR_e of PNIPAM/PEG hydrogels decrease with increasing radiation dose, and their swelling performance decreases with increasing radiation dose. However, the hydrogel strength for the low q_0 was small at lower radiation doses, and applicable at the 8-kGy radiation dose, even though the larger *SR* was owing to that water molecules can easily enter the hydrogel inner. The q_0 increases with the radiation dose, and more chemical bonds connecting between molecules resulted in molecular force became larger. The whole system of hydrogels became closed with increasing radiation dose. Small molecules like water were unlikely to enter the hydrogel inside, thus decreasing the *SR* of hydrogels. Hydrogels were prone to brittle fracture owing to excessive q_0 at the radiation dose of more than 22 kGy, so radiation dose preparing PNI-PAM/PEG porous hydrogels was selected as 15 kGy.

The phase transition properties of temperature-sensitive hydrogels are expressed by the LR_w under different temperatures. The greater the LR_w was, the more the phase transition was. Fig.3 shows the de-swelling kinetics curve of PNIPAM/PEG_{6000} hydrogels, the average LR_w of hydrogels with PEG_{6000} was about 70% within 0.5 h, but the LR_w of PNIPAM

hydrogel was only about 15%. When shrinking, the water in the PNIPAM/PEG_{6000} hydrogel could freely squeeze out. When moving to the 50°C water, the PNIPAM hydrogel was exposed to the high temperature environment, the phase separation firstly occurred and the hydrogel chains contracted. Hydrogel dehydration began from its outside surface to the internal. Dense layer formed on the surface of PNIPAM hydrogels. The water in hydrogels could not fully spread through the dense layer due to the cumulative diffusion. Therefore, the LR_w of hydrogels without PEG was very smaller than that of porous hydrogels. The hydrogel pores had a great impact on its de-swelling rate. On contracting, there were a large number of air bubbles on the surface of PNIPAM hydrogels, but few air bubbles on the surface of PNIPAM/PEG_{6000} hydrogel. When reaching swelling equilibrium, the hydrophilic amide group (-CONH-) and hydrophobic isopropyl group (-$CH(CH_3)_2$) in the network of PNIPAM hydrogel achieved a balanced state. At the outside temperature of about 50°C, the hydrophobic interaction was dominant. When the general PNIPAM hydrogel was put into hot water, its surface firstly lost water, the phase separation occurred and dense layer formed on the surface to prevent the water seepage, there were a lot of tiny bubbles on its surface due to gradually increasing internal pressure. But a dense layer on the porous PNIPAM/PEG_{6000} hydrogel did not form with its contracting. In the de-swelling, the porous hydrogel structure was conducive to extruding water out, and has little bubble on its surface.

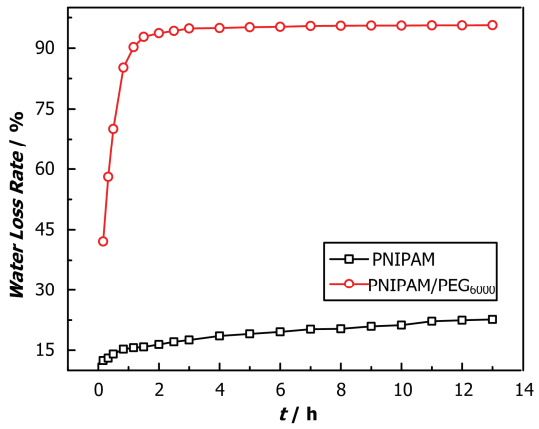

Fig.3 The de-swelling kinetics of PNIPAM/PEG hydrogel at radiation dose of 15 kGy.

The relationship of SR_e of PNIPAM/PEG_{6000} hydrogel with temperature at different radiation doses is shown in Fig.4, the SR_e decreased with increasing temperature below LCST, and was similar up to 37°C. The radiation doses have little effect on the LCST up to about 37°C. The PNIPAM/PEG_{6000} hydrogel had the heat shrinkable behavior by its temperature sensitivity.

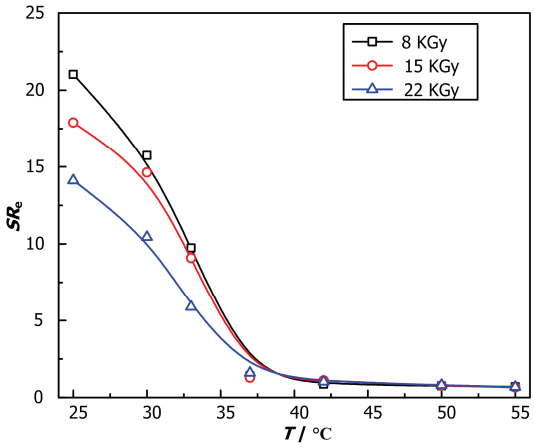

Fig.4 The relationship of SR_e with temperature for PNIPAM/PEG_{6000} hydrogel under different radiation doses.

3.3 Thermal analysis of hydrogels

The chemicophysical properties of hydrogels are determined by the interaction of cross-linked network of polymer with water. It is generally believed that there are three states of water in the hydrogels, that is, the bound water, the free water (frozen water) and the interstitial water[27]. From perspective of hydrogen bond structure and movement state, the bound water is due to the hydrophilic group of the polymer network, forming a whole entirety with the polymer chain. The free water exists in the larger cyberspace of polymer network. On forming hydrogen bonds, it had the similar ability with the general free water. The interstitial water is in the state between the bound water and free water.

When shrinking with increasing temperature, the water in the network of hydrogels loses gradually, and the free and interstitial water are squeezed out except for the bound water. So the LR_w decreases with increasing swelling time until its equilibrium value.

Similar with ice melting, the DSC curves of PNIPAM/PEG hydrogels at the different radiation doses show that an endothermic peak appeared in the vicinity of 0°C, indicating that the hydrogels formed ice phase at low temperature, but its melting

temperature was lower in hydrogels than in pure water. Assuming the melting enthalpy in hydrogels of frozen water was the same as that of pure water at 333.7 $J \cdot g^{-1}$, the content of frozen (W_f) or non-frozen water (W_{nf}) could be calculated by Eq.(6) using their enthalpy (peak area) near 0°C (Fig.5).

$$W_f=[\Delta H_g/\Delta H_0]\times 100\% \quad (6)$$

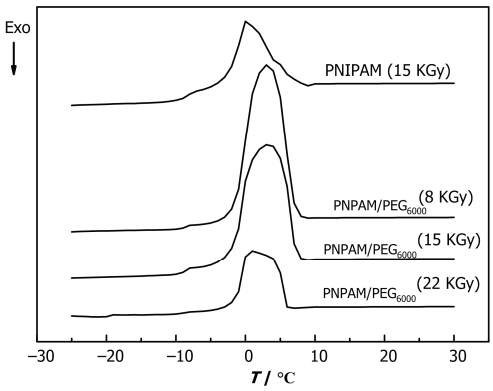

Fig.5 DSC curve of the PNIPAM/PEG hydrogels at different radiation doses.

The water content in different hydrogel states is shown in Table 2. At 0°C, the hydrogel enthalpies with increasing temperature was less than that of pure water due to their different states, indicating the enthalpy change in the frozen water. The frozen water was greater in PNIPAM/PEG_{6000} hydrogel than in the PNIPAM hydrogel at radiation dose of 15 kGy. The endothermic peak of PNIPAM/PEG_{6000} hydrogel shifted to low temperature and decreased with increasing radiation dose, its frozen water decreased continuously. In other words, non-frozen water increased. Because the frozen water decreased with increasing radiation dose, the network density of hydrogel chains increased with radiation dose, resulting in the swelling its low degree, thus, the frozen water in the entire network decreased. The experimental results were consistent with the relationship of SR_e in deionized water with time at different radiation doses.

Table 2 The content of different types of water in hydrogels

Sample	PNIPAM(15 kGy)	PNIPAM/PEG_{6000}(8 kGy)	PNIPAM/PEG_{6000}(15 kGy)	PNIPAM/PEG_{6000}(22 kGy)
θ_0/°C	–10.7	–8.7	–7.5	–7.7
θ_t/ °C	–0.6	2.7	2.7	0.7
Δθ/°C	8.9	10.2	9.1	6.8
R_{fw}	Slow	Slow	Faster	Fast
H_0/ $J \cdot g^{-1}$		333.7		
H_g/ $J \cdot g^{-1}$	140.2	244.2	229.3	213.9
W_f/ %	42.0	73.1	68.7	64.1
W_{nf}/ %	58.0	26.9	31.3	35.9

Note: $W_{nf}=1-W_f$, θ_0 is the temperature of starting melting, θ_t is the peak temperature.

The degradation of both PNIPAM/PEG_{6000} hydrogel and PNIPAM hydrogel has only a significant loss step, as shown in Fig.6. The DTG curve shows that the PNIPAM/PEG_{6000} hydrogels have little reduction in thermal stability, indicating that the porous hydrogels introducing the PEG6000 did not change the thermal degradation mechanism of PNIPAM matrix.

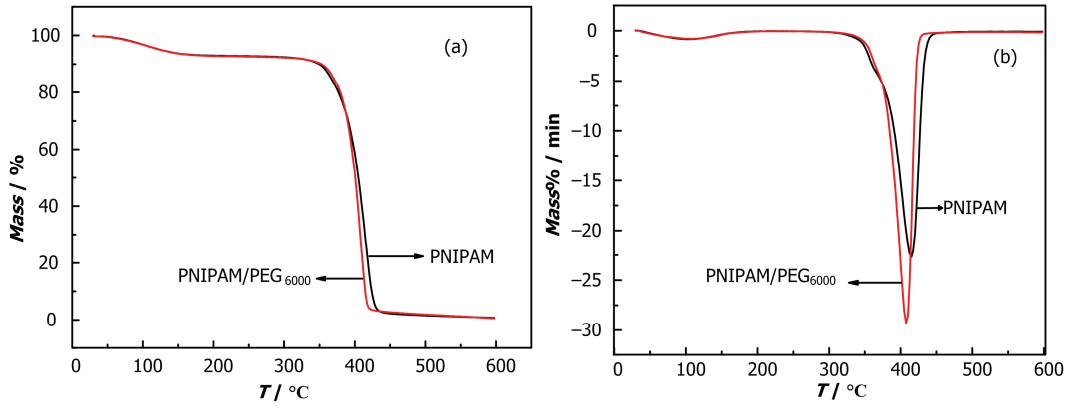

Fig.6 TG and DTG curves of PNIPAM/PEG hydrogels.

3.4 SEM analysis of hydrogels

When hydrogels are dried in normal conditions, their large changes of volumes cannot collapse the pore structure due to the loss of water. After hydrogels are freeze-dried, the polymer chains are highly bound, and the system of polymer network and water is in the solid-state. When water is excluded by the sublimation, the internal structure of the polymer network still maintained without causing large extent deformation. Therefore, freeze-drying method after quenching is taken in the experiment. After freeze-drying hydrogel, its structure morphology of the cross-section region can be directly observed by SEM. Fig.7 shows the SEM images of the cross-section of PNIPAM hydrogel and porous PNIPAM/PEG_{6000} hydrogel by quenching in liquid nitrogen. The surface of hydrogels without pore-forming agent was denser, and formed only the folds in the freeze-drying process. Lots of obvious pores appeared in PNIPAM/PEG_{6000} hydrogel with the pore-forming agent, providing channel for water and water-soluble substances, such as nutrients, metabolites through out of hydrogels.

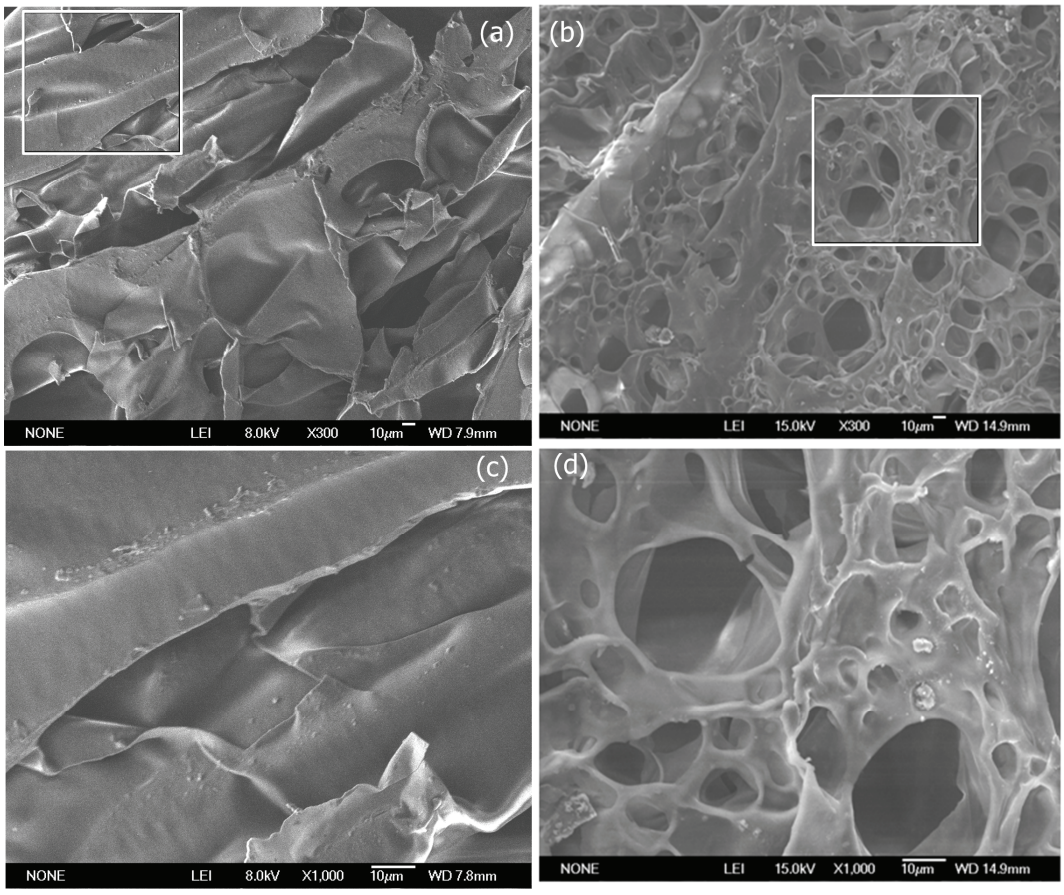

Fig.7 SEM imagines of PNIPAM hydrogel (a,c) and PNIPAM/PEG_{6000} hydrogel (b,d).

4 Conclusions

The PEG molecules as pore-forming agent in the cross-linked polymerization did not participate in the reaction. The SR_e reduced with increasing radiation dose. The LCST around 37°C was little affected by different radiation doses. The frozen water of PNIPAM/PEG_{6000} hydrogel was greater than that of PNIPAM hydrogel at 15-kGy radiation dose, and decreases with increasing radiation dose. This may be appropriate as release polymer systems in pharmaceutical formulations.

References

1 Karg M, Hellweg T. Curr Opin Colloid In, 2009, **14:** 438–450.

2 Wang Q, Zhang J P, Wang A Q. Carbohydr Polym, 2009,

78: 731–737.
3 Lai F K, Li H. Mech Mater, 2011, **43:** 287–298.
4 Tajima H, Yoshida Y, Abiko S. Chem Eng J, 2010, **156:** 479–486.
5 Huang S H, Tsai C, Wu C W. Sensor Actuat A-Phys, 2011, **165:** 139–146.
6 Peppas N A, Bures P, Leobandung W. Eur J Pharm Biopharm, 2000, **50:** 27–46.
7 Zhang X Z, Zhuo R X, Cui J Z. Int J Pharm, 2002, **235:** 43–50.
8 Keir N, Woods C A, Dumbleton K. Contact Lens Anterior Eye, 2010, **33:** 189–195.
9 Varshney L. Nucl Instrum Meth B, 2007, **255:** 343–349.
10 Liu K M, Li Y B, Xu F L. Mater Sci Eng, C, 2009, **29:** 261–266.
11 Abdolijalil K H, Naser M, Mehdi R. Aesthetic Surg J, 2008, **28:** 139–142.
12 Lu X H, Sun M Y, Barron A E. J Colloid Interface Sci, 2011, **357:** 345–353.
13 Crompton K E, Goud J D, Bellamkonda R V. Biomater, 2007, **28:** 441–449.
14 Zhang Y T, Zhang L, Chen H L. Chem Eng Sci, 2010, **65:** 3199–3207.
15 Chen J, Liu M Z, Zhang N Y. Sens Actuators, B, 2010, **149:** 34–43.
16 Strachotová B, Strachota A, Uchman M. Polym, 2007, **48:** 1471–1482.
17 Gallego G, Monleón M, Gómez J L. Eur Polym J, 2010, **46:** 774–782.
18 Topuz F, Okay O. React Funct Polym, 2009, **69:** 273–280.
19 Aaron D L, Anna K B, Themis R K, *et al*. J Biomed Mater Res A, 2011, **96:** 621–631.
20 Zamani A Z, Henriksson D, Taherzadeh M J. Carbohydr Polym, 2010, **80:** 1091–1101.
21 Pasc A, Gizzi P, Dupuy N. Tetrahedron Lett, 2009, **50:** 6183–6186.
22 Kato N, Gehrke S H. Colloids Surf B, 2004, **38:** 191–196.
23 Wachiralarpphaithoon C, Iwasaki Y, Akiyoshi K. Biomater, 2007, **28:** 984–993.
24 Casimiro M H, Botelho M L, Leal J P, *et al*. Rad Phys Chem, 2005, **72:** 731–735.
25 Xue W, Champ S, Huglin M B. Eur Polym J, 2004, **40:** 467–476.
26 Charlesby A. Atomic Radiation and Polymers, New York, Pergamon Press, 1960, 68.
27 Ping Z H. Polym, 2001, **42:** 8461–8467.